Ceramic-Polymer Additive Manufacturing System for Ultrasound Transducers

Mark Cheverton, Prabhjot Singh, L. Scott Smith, Kwok Pong Chan,
James A. Brewer, Venkat Venkataramani
GE Global Research, Niskayuna NY 12309
cheverto@research.ge.com

Abstract

A modified multi-layer lithography process is used to additively manufacture high-resolution netshape ceramic structures by photopolymerizing a ceramic-polymer slurry using structured light patterns. This paper will discuss the development of a low-cost, high speed manufacturing process method for the fabrication of piezoelectric ceramic transducer elements in the 1-25 MHz frequency range. The key considerations in the development of the process including the selection and optimization of slurry materials for the deposition of PZT 5H materials, optical exposure parameters, debinding/sintering profiles, process monitoring, and post manufacturing processing. Ongoing work includes improvements to the materials properties, improved throughput and geometric fidelity.

Introduction

Ultrasound transducers constitute a key sensor technology for both medical and non-destructive testing. Ultrasound has become the most common medical imaging procedure because the process is fast, avoids ionizing radiation, is relatively portable, and uses inexpensive equipment. For the non-destructive evaluation of high value metal, ceramic, and composite parts, the use of ionizing radiation is less of a concern, while the other characteristics still apply. In both of these applications, the ability to efficiently generate high quality ultrasound beams in the inspected body is critical. For medical imaging that means the use of phased array technology where individual transducer elements, and time delays are used to form the transmitted and received beams. This same technology is used in some non-destructive testing systems. However, there is also a significant use of single element ultrasound transducers where the use of 1-3 composite transducer structures[1] improves beam quality. So in both applications, arrays or composites, the fabrication of small pillar-like structures is central to the device technology. Conventional technology, based on dicing plates of piezoelectric and other acoustic impedance matching and backing materials, has been functionally effective. Because it is based on a serial and sequential process, it does not scale well to higher production volumes and tends to be slow, or equivalently requires parallel capital equipment investment. Additive manufacturing provides a novel alternative approach to fabricating ultrasound transducers.

Prior Work:

Extensive prior work on the layered deposition of various structural and electrical ceramic materials has been reported in literature. Several modes of layer creation have been researched. These include

extrusion of semi-molten thermoplastic-ceramic filament material[2-3], photocuring of ceramic-polymer slurries[4-8] inkjet of wax-ceramic[9] mixtures etc. Additionally, micro-molding techniques have also been researched[10]. [11] summarizes various micro-layered manufacturing processes for ceramic fabrication. In the context of photocurable ceramic-polymer layered deposition processes, key process considerations include the ability to:

- Formulate low-viscosity slurry materials that can be spread to form 10-100 micron thick layers with high consistency. This is usually accomplished by suspending fine ceramic particles with stearic dispersants in a photocurable (acrylate, epoxy etc) monomer
- Photocure the slurry layers and form cross-linked polymer chains within and across layers using a high intensity, UV-rich light pattern. This pattern could be formed by a laser or a digital spatial light modulator. The refractive index of the slurry constituents, the incident light spectrum and the particle size distribution usually affect the depth of cure and the resolution of the patterns
- Sinter the ceramic-polymer green parts to high density using carefully controlled thermal cycles in the appropriate environmental conditions

Relatively limited work has been reported on the photocuring of lead-based piezoceramic slurries[12-13]. This is largely due to two factors; first, the high refractive index of such ceramic materials, which causes light to scatter preventing cross-linking through the thickness of the slurry layers; second, the sintering of lead-rich piezoceramics is difficult due to the volatility of lead at high temperatures leading to poor electromechanical properties in sintered structures. The relatively high surface area of netshape green parts amplifies this problem. In the following section we discuss the experimental methods used to netshape manufacture of lead zirconate titanate (PZT) parts in clinically relevant geometries (size and feature fidelity).

The paper is organized as follows: system architecture with an emphasis on components and challenges encountered & the material system will be described. Thereafter, the manufacturing process will be discussed, and finally the post processing with lessons learned.

Manufacturing Process:

The manufacturing process can be summarized with four steps, the dispensing of the photo curable material, the spreading of the material, the exposure of the material, and finally the removal of all uncured material. This process is summarized in figure 1 below:

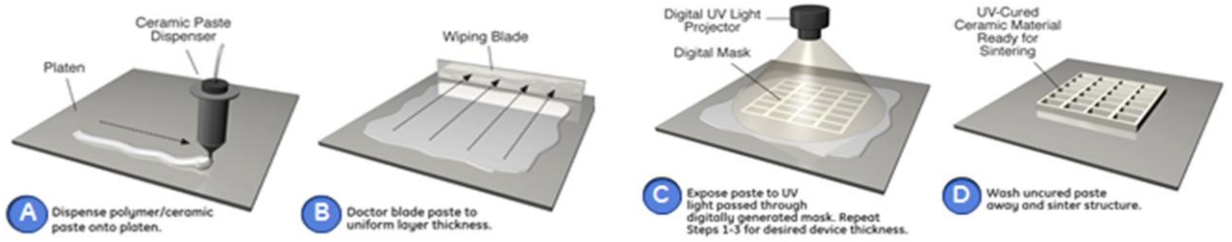

Figure 1 – Additive process for manufacture of ultrasound transducers.

System architecture

A key feature of ultrasound transducers is their constant cross sectional structure, which make a layerwise additive process using a fixed mask for patterning very attractive. The system built at GE's Global Research Center focused on this layerwise process, using UV curable materials. The system uses high resolution x/y/z stages, automated dispenser to deposit a controlled amount of material, a high intensity UV light source, and a chrome-on-glass mask with the pattern to be written, and multiple cameras to monitor the manufacturing process and detect problems if they occur during build. The entire system was integrated with custom software developed in LabVIEW. The following system categories will be discussed in turn: material system, light source, material deposition, material spreading, motion control and the software system, process monitoring, and part post processing.

Material system:

Starting materials & Slurry Preparation

The current UV-curable PZT formulation was prepared using PZT powder as the ceramic filler and a diacrylate photocurable resin binder with an appropriate concentration of a photoinitiator. A stearic dispersant was used to promote the dispersion of PZT particle within the organic resin.

The ceramic slurry formulation with 80wt% of ceramic content was prepared by mixing the constituents in a planetary mixer for 2 hrs using grinding media to break agglomerates in the ceramic powder. Isopropanol was added to the mixture to adjust the viscosity of the slurry. Thereafter the slurry was transferred to a 30cc EFD syringe cartridge for use with the deposition system.

A significant effort went into developing a slurry with specific flow characteristics of viscosity ~ 10 poise at shear rate between10 s^{-1} to 100 s^{-1} (typical shear rate range of our equipment). This involved mixing various components with zirconia media balls in a high speed planetary mixer to reduce the particle size. A viscosity profile of PZT slurry was shown in figure 2. The slurry exhibits a shear thinning behavior of a non-Newtonian fluid. If the material was mixed and allowed to sit for longer than half a day, then the material tended to not flow or spread very well, and would not make acceptable parts.

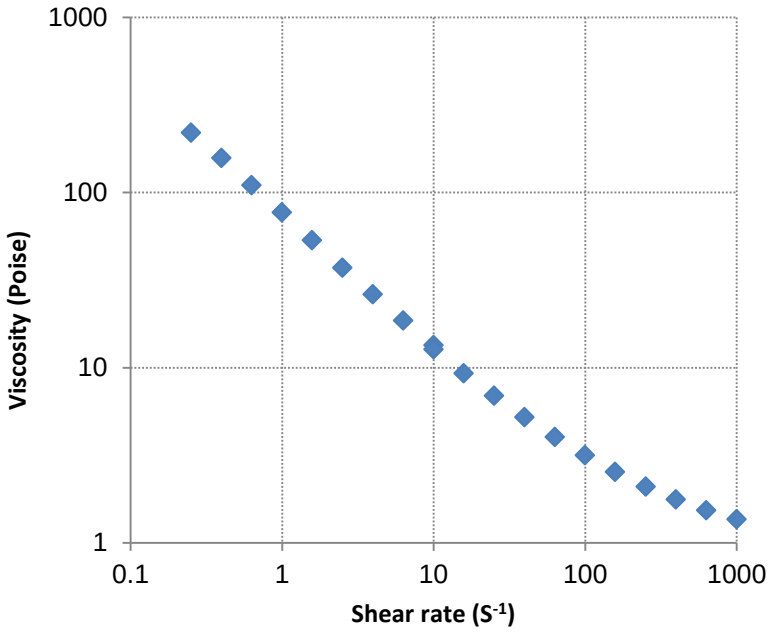

Figure 2: Viscosity of the photosensitive PZT-diacrylate slurry

The amount of PZT and polymer (HDODA) was determined mathematically, such that the volume fraction of PZT would be 38%-40% after IPA evaporated. Photoinitiator amounts were determined empirically by testing fixed exposure times with varying amounts of photo initiator and assessing the level of adhesion between successive layers. With too little photo initiator, the parts do not cure sufficiently and fall apart when cleaning the uncured slurry out of the green part. With too much photoinitiator, the scattering increased, decreasing pattern resolution with small features becoming merged together.

Light source:

Knowing that there would need to be high solids loadings in order to achieve the densities necessary for ultrasound transducer applications, the first consideration in selecting the light source was high power. LED fiber light sources were considered, but with the desire to operate in the UV range, there appeared to be limited options to achieve high power and relatively collimated light output. As a result, the Newport model 92292 UV solar simulator was selected for use in this system. This light source yielded a total output of 150 mW/cm^2 in the UV-A range and 75 mW/cm^2 in the UV-V range. Communication to this light source was done via RS232.

Material deposition:

Material deposition was performed using a pneumatic pump, Nordson EFD Ultima model as well as with Aerotech translation stages, integrated using LabVIEW. This system used air pressure to dispense material from a 22 gauge syringe tip attached to a 30cc tube. To activate the pump, a TTL signal was used, the high state turning on the pump and allowing it to dispense, and the low state turned off the pump.

The slurry was dispensed as a bead across the substrate, with the location of the bead determined experimentally so that the material would be positioned properly. The system would move to the start of the bead, and then the pump turned on. The motion control system them moved the substrate under the dispenser so that a bead was deposited parallel to the doctor blade. When the system reached the end point, the dispenser was turned off. The volume of material being deposited was controlled by controlling the speed of the stage as it traversed under the dispenser. A slower speed allowed for more material to be deposited. A camera system was designed & installed to detect flow stoppages in the syringe. It was observed that stoppages in the build led to subsequent delaminations in the part.

Material spreading:

The dispensed bead, as described above, was spread using a stainless steel doctor blade. This doctor blade was carefully leveled to the substrate using micrometers so that the gap on both ends of the doctor blade were the same. The vacuum chuck which held the glass substrate, upon which everything was built, had to also be leveled to the blade, so that the gap between the blade and the substrate would be the same at the beginning and the end of the wipe. This leveling was done with thin shim material so that the gap at the beginning and the end of the wipe would be within 20 um or better.

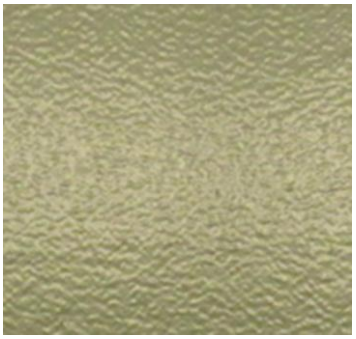

Figure 3 – surface finish with a wipe speed of 0.5 mm/s

It was found to be important to level the vacuum chuck with the vacuum on, as the glass substrate changed shape slightly, likely due to the non-flattness of the vacuum chuck. In any event, if the leveling was done with the vacuum on, and then parts were built with the vacuum off, or vice versa, there was a chance of the doctor blade colliding with the glass substrate, causing the process to fault and stop.

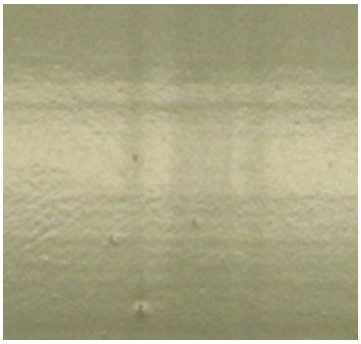

Figure 4 – surface finish with a wipe speed of 3 mm/s

One of the challenges that was discovered when conducting experiments on the spreading of the material was the relationship between surface finish and wipe speed. Initially, the wipe speed was set to a small number, in the neighborhood of 0.5 mm/s. This was done so that the wiping would not destroy any of the subsurface features that had already been printed. However, it was found that the slow speed yielded a poor surface finish, as shown in figure 3. In comparison, figure 4 shows the surface finish with a wipe speed of 3 mm/s. These images were acquired by looking at the specular reflection of a structured light. In figure 3, the dark stripes cannot be seen, but on figure 4, the dark stripes are clearly visible. Wipe speeds greater than 3 mm/s were tried, but speeds greater than 3 mm/s were found to be detrimental to already printed subsurface structures. To document the

quality of each layer, a camera was installed in the system to take a picture of every layer before exposure. This allowed analysis of the quality of the wipe to detect problems like not dispensing enough material, or viscosity changes causing insufficient volumes of slurry being dispensed, which in turn caused incomplete layer coverage. More information about the surface imaging camera will be discussed in the process monitoring section.

Custom control software

The control of these stages was done using LabVIEW. The software was developed with experimentation in mind, but it also had a manufacturing setting, so that control of the system could be limited and operation could be done by individuals with only basic training on how to operate the system. The software was written with a standard-state machine architecture, with an event structure at the beginning of the state machine for experimentation. The series of steps in the software were the following: dispense, wipe, clean, evaporate solvent, and expose.

Dispense - In the dispense step, the system moved to the start of the bead that would be deposited. This location was stored in an ini file that could be easily edited with a simple text editor, or it could be modified with tools built into the software. The start point, the end point, and the velocity of the traverse were defined in the ini file, with lower velocities allowing the system to deposit more material and high velocities for less material. The speed of the translation stage, the air pressure used on the pump, and the needle size were all factors that were optimized to get the right amount of material deposited so that there was complete coverage without too much excess slurry left over at the end of the wipe.

A camera, LED backlight, and mirror were positioned so that the dispense could be monitored. The LED backlight and camera were positioned on opposite sides of the dispense stream, with the mirror used to fold the path so that it fit within the footprint of the system.

Wipe - After dispensing the bead, the stages moved so that the doctor blade was just behind the bead of slurry. Typical layer thicknesses for this process were 20 um. As a result, the doctor blade had to be very close to the substrate or previous layers. To mitigate the risk of the doctor blade overshooting its position and colliding with the substrate, the system moved to within 1 mm of the target height, and then very slowly approached the final position at approximately 0.1 mm/s. This slow approach eliminated any collisions between the doctor blade and the previously printed layers.

The start point of the wipe, the end point of the wipe, and the wipe speed were defined in the build parameters, in an ini file. The engineer running the system could modify these parameters with a text editor, or use on-screen tools to modify these settings.

A critical concern with the wipe was found to be the wipe speed, not just because of surface quality, but also with respect to current draw on the stages. If a very low wipe speed was used, the z-stage would draw excessive current in order to keep its height constant, frequently causing

unrecoverable over-current faults when the average current draw went over some threshold set in the Aerotech parameter file, causing the process to stop. It was found that the higher wipe speeds not only produced a better surface finish, but also reduced the number of over-current faults with the stages.

Clean – After spreading the material over the substrate, the system moved to a location such that a sponge was positioned at one end of the doctor blade. The sponge was then wiped across the doctor blade, to clean any residual slurry left on the blade. If this step was skipped, then one ran the risk of leaving slurry on the blade, and having the slurry cured by collateral exposure from the UV light, destroying the nice, flat surface of the doctor blade. As a result, this cleaning step was performed immediately after each wipe.

Evaporate solvent – Before the exposure, excessive solvent was removed from the part by moving the part in front of a fan for one minute. During that minute, the fan would be turned on, via LabVIEW, and the residual solvent that was added to the slurry, to lower the viscosity so that it could be dispensed easily, would evaporate, allowing a small amount of shrinkage. During this step, an LED line light would be turned on, and the light would be emitted with a grazing incidence angle, parallel to the surface of the material. A camera would capture an image from above; the glancing lighting allowing topological features to be highlighted and captured by the camera for later analysis. Images from this camera can be seen in figure 7 and 8.

Expose – After the evaporation step, the stages would move the sample under the light source for exposure. Typically, twenty base layers, without any pattern, would be exposed into the material. After those base layers were complete, then the desired pattern would be exposed by positioning a chrome-on-glass mask from Advanced Reproductions, Inc. between the sample and the light source. This mask was held on a translation stage from Velmex, and moved into position after the base layers were complete.

It was important to position the uncured layer as close to the mask as possible, in order to get sharp shadows and good size definition. The spacing chosen for this process was 0.25 mm. As a result, the parallelism between the mask and the substrate was very important. A great deal of effort was put into designing a fixture that would hold the mask but allow enough degrees of freedom to easily get it level to the substrate while still being strong enough so as it would not droop over time. A two axis kinematic mount with micrometers was selected from Thorlabs. The micrometers made leveling much easier than using shims.

With such a small gap between the mask and the uncured material, collisions were problematic. Therefore, as described above, the stage would move the substrate to within 1 mm of the final exposure position, and then approach the desired exposure height with a very low velocity. If a collision did occur, then uncured slurry would get on the mask, and then be cured to the mask by the UV light. When this would happen, it was necessary to remove the mask completely, soak it in acetone overnight, then glue it back to its frame again, remount it to the Velmex stage, and relevel it to the substrate.

Once the exposure step was complete, the system would then repeat the process, moving the stage to the start of the dispense step, and go through all the steps again. The wipe and the expose steps had to track the height of the part, and change their z-position to account for all previous layers, so that the height of the uncured slurry was always held constant, even though the z-height of the stage was not.

To enable experimentation, all of the above steps could be run individually using preset parameters. As a result, when new materials were being developed, it was common for the researcher to do a test dispense, just to see how the material would flow, and then perhaps do a test wipe, just to see the flow dynamics and surface finish. The screen for the control software is shown on figure 5.

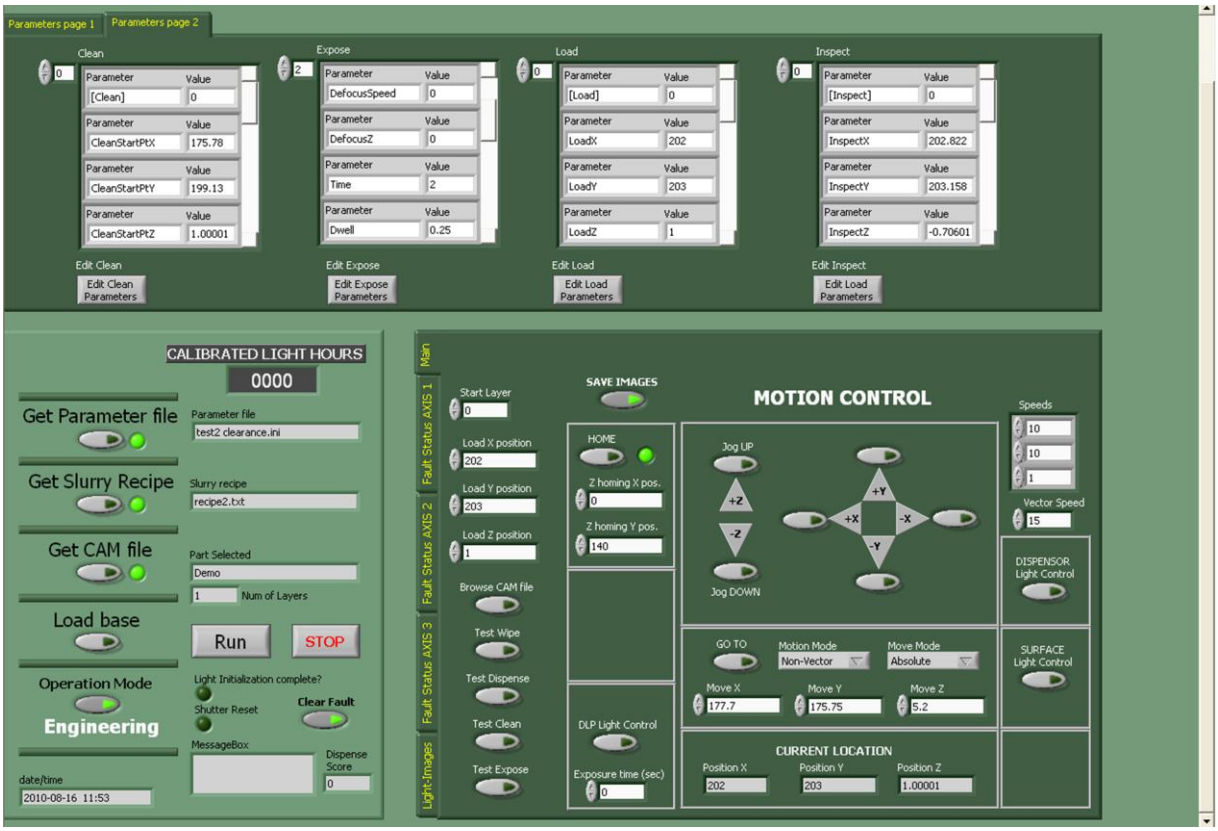

Figure 5 – screen shot of control software

Process monitoring:

Two cameras were integrated into the system, one to monitor the dispense, and a second to monitor the surface quality of the layers just before the exposure. The goal of these cameras was to notify the operator about a problem early in the process, so that corrective actions could be taken to save the build, or terminate the build and start a new one. Because these builds could sometimes take many hours to complete, it was important to have the capability to monitor the process and have automated decisioning built into the software system.

Dispense Camera:

This camera looked at the dispense stream and verified that something was dispensed. This was done by putting an LED backlight on one side of the dispense stream, and the camera on the other, with a mirror on the camera side to fold the optical path, making the camera fit within the footprint of the system. The system would take a picture of the dispenser before it was actuated, then take a picture during dispensing, and subtracting the two images so that only the slurry stream could be extracted from the image. Because the slurry is opaque, it appeared black in the image, with the background (the LED backlight) being saturated at a grey value of 255. With such a large contrast, it was easy to detect the stream and verify that the system was actually dispensing slurry.

Nozzle clogs were detected and the system would attempt to re-start multiple times. Once the needle on the dispenser was changed and a successful dispense was done, the system would then send an email to the team notifying them that the process had been successful restarted and the problem solved. If the needle was replaced within twenty to thirty minutes and the process continued, then the build would still be successful. Excessive solvent vaporization and water uptake were suspected to be the two leading causes of dispense failures. Figure 6 shows images captured from the dispense camera. The thicker section at the top of figure 6 (a) is the actual nozzle, and the thick black line at the bottom off the image is part of the drip cup.

Figure 6: a – image of the slurry stream during deposition, b – detected stream after image processing

Surface camera:

A megapixel camera was positioned over the sample with a working distance of approximately 18 inches so that the camera was out of the way of the operator during loading and unloading of the system. An LED line light from CCS-America was positioned so that the light from the line light was focused across the top layer of the sample, with the light collimated parallel to the surface. This grazing lighting position was used to highlight one side of a bump on the surface of the part being build, and cause a shadow on the back side of the bump. In this way, the lighting highlighted topological features in the slurry layer.

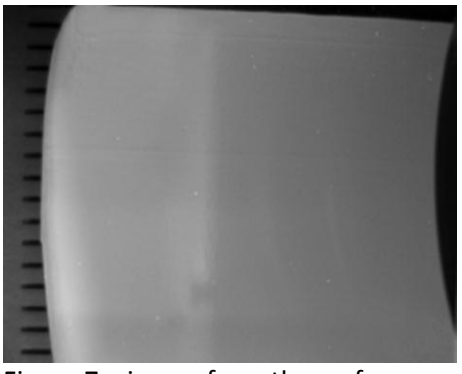

Figure 7 – image from the surface camera.

Just before exposure, the motion stages were used to place the deposited layers underneath the camera, defined in the build parameters. LED lights were turned on and an image of the layer was taken and saved for analysis post-build. It was possible to detect topological anomalies and make decisions, like re-wipe the layer, or put on more slurry and wipe again, or even abort the build, however these features were tested but never implemented into the final software version. Figure 7 shows an image of the sample surface just after the wipe but before the exposure on layer 12.

There are few features to be seen in this image, however, as this build continued, the slurry's viscosity increased, making the dispense put down too little slurry, creating a topological feature at the end of the wipe. These features can be seen in figure 8.

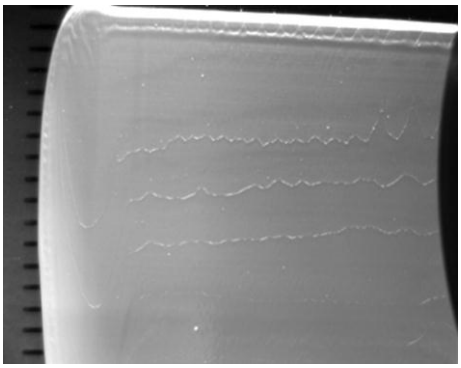

Figure 8 – image from the surface camera.

This surface camera proved essential in understanding the kinetics of the wiping process, and the effects that the sub-surface structures can cause on the fluid dynamics of the wiping process.

Post processing:

Cleaning:

The most challenging part of the process was the cleaning of the uncured slurry from the part, without damaging any of the cured features. For the ultrasound transducers being manufactured on this additive system, a series of bars were printed, as shown in figure 9. The typical dimension of the bars were 250 um wide with a 60 um kerf in the green state. The image in figure 9 is a post sintered structure.

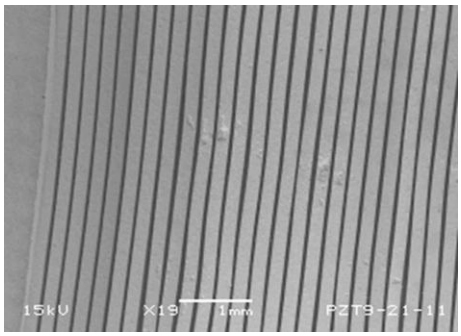

Figure 9 – micrograph of ultrasound transducer ceramic green parts.

Upon completion of the build process, the build plate (glass) was removed from the vacuum chuck. Excess uncured slurry was removed with a spatula, then the part, still on the glass substrate, is put in an ultrasonic bath to remove excessive slurry. Delaminations and broken features were observed during the cleaning process. Process yield was ~40%. Parts were then dried in an oven.

Sintering:

A 2-stage densification process was developed to obtain high-density ceramics. In the first stage, the organic constitutents of the part were pyrolyzed in an oxygen environment using a carefully designed thermal cycle based on the thermogravimetric analysis of the photocurable binder and the surfactant. This is essential to avoid thermally shock which leads to part breakage. Temperature in the first stage was restricted to 700C to avoid lead loss. In the second stage, the part was placed on platinum foil and the sealed in a magnesia crucible with extra piezoceramic source powder. Magnesia sintering furniture was selected to minimize reactions with lead which is volatile above 700C. The extra source powder was added to ensure a positive vapor pressure of lead during sintering. A Zircar Zirconia box furnace was used to sinter the part. A uniform heating rate of 1 degree/minute was used to prevent thermal shock and obtain isotropic shrinkage. Density was measured using the Archimedes principle in a water bath of known temperature. Special setters were created to ensure that the features in the ultrasound transducer ceramic stayed straight (Figures 10 & 11).

Figure 10 – transducer after

Figure 11 – transducer after sintering improvement w/ setters

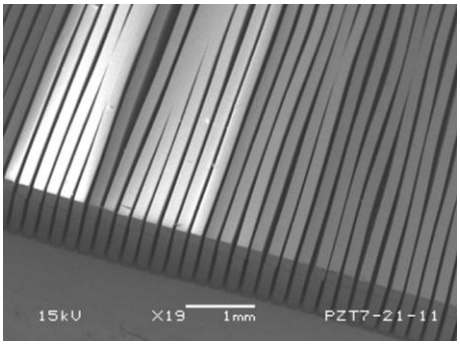

Figure 12 – sintered transducer without setter

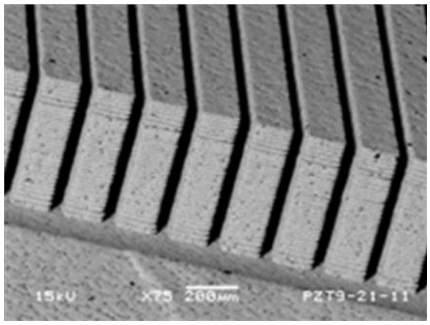

Figure 13 – sintered transducer with setter

Transducer performance:

Parts produced by this process are in the 95%-98% dense, with a grain size of 2-3 microns. Lead loss during sintering was less than 0.5%. This was determined by measuring the weight of the parts before and after sintering. The electromechanical coupling coefficient (kt) was between 0.52-0.53 with a dielectric constant of 2000. The resulting probe operates at a center frequency of 2.x MHz.The piezoceramic composite was processed into a convex transducer.

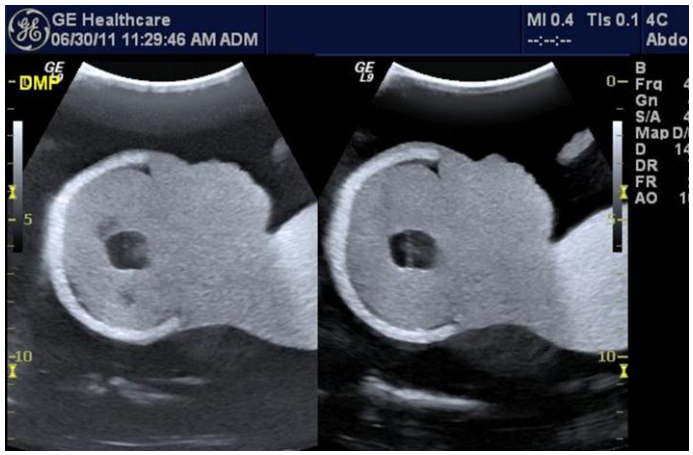

Figure 14 – ultrasound images of a fetal phantom. The image on the left is from the transducer build by the additive process described, and the image on the right was from the commercial ultrasound system.

The ceramic wafers were built into a convex transducer array and tested on a fetal a phantom. The images from the GE constructed ultrasound transducer were compared to images captures from a commercially available ultrasound system. The images from these tests can be seen in figure 14.

Conclusion

Through the use of an additive process, it was demonstrated that ultrasound transducers could be manufactured with high resolution features that yield images comparable to commercial systems. Slurry chemistries and cleaning processes were developed to optimize the yield of the manufacturing process. In addition, machine vision based process monitoring was integrated into the custom system to monitor the process, so that when problems occurred, operators could intervene quickly rather than waiting for the long build to finish, only to yield a failed part. Future work on this process will include further optimization of the slurry chemistry & improvements to the deposition set-up .

This work was supported by Award Number RC2EB011439 from the National Institute of Biomedical Imaging And Bioengineering. The content is solely the responsibility of the authors and does not necessarily represent the official views of NIBIB or the NIH.

References

1. W.A. Smith The Role of Piezocomposites in Ultrasonic Transducers. Proceedings of the 1989 Ultrasonics Symposium 755-766.
2. Safari, M. Allhverdi, E.K. Akdogan, *Solid freeform fabrication of piezoelectric sensors and actuators*, J. of Materials Science, Vol. 41, pp. 177-198, 2006.
3. Safari, M. Ebrahimi, S. Turcu, A. Hall, R. Brennan, N. Hagh, *Layered manufacturing for prototyping of novel transducers*, In proceedings of Ultrasonics Symposium, 2002.
4. X. Zhang, X. N. Jiang, C. Sun, *Micro-stereolithography of polymeric and ceramic microstructures*, Sensors and Actuators A (Physical), Vol.A77, (no.2). pp149-56, 1999.
5. Bertsch, S. Jiguet and P. Renaud, *Microfabrication of ceramic components by microstereolithography*, Journal of Micromechanics and Microengineering, Vol. 14, pp. 197-203, 2004.
6. G. T-M. Chu, G. A. Brady, W. Miao, J. W. Halloran, S. J. Hollister, D. Brei, *Ceramic SFF by direct and indirect stereolithography*, Solid Freeform and Additive Fabrication, MRS Symposium Proceedings, Vol. 542, pp. 119-123, 1999.
7. T. Chartier, R. Penarroya, C. Pagnoux, and J. F. Baumard, *Tape Casting Using UV Curable Binders*, Journal of the European ceramic society, vol. 17, pp. 765-771, 1997.
8. H., Chabok, C. Zhou, S. Alagha, C. Yong, Q. Zhou, K. K. Shung, *Development of a digital micro-manufacturing process for high frequency ultrasound transducers*, Ultrasonics Symposium (IUS), 2010 IEEE pp.666- 669, 11-14 Oct. 2010.
9. T. Ang and B. Derby, *Ink-jet printing and sintering of PZT*, Journal of the American Ceramic Society, Vol 88:8, pp. 2053-2058, 2005.
10. S, Cochran, A. Abrar, K.Krik, D. Zhang, T. Burton, B. Su, and C. Meggs, *Net-shape ceramic processing as a route to ultrafine scale 1-3 connectivity piezoelectric ceramic-polymer composite transducers*, IEEE Ultrasonics Symposium, Volume 3, Issue 23-27, pp: 1682-1685, 2004.
11. Bertsch, S. Jiguet, P. Bernhard, P. Renaud, *Microstereolithography: a Review*, In Proceedings of Materials Research Society Proceedings, Vol. 758, Boston, MA, 2002.

12. X. N. Jiang, C. Sun, X. Zhang, B.M. Xu and Y.H. Ye *Microstereolithography of lead zirconate titanate thick film on silicon substrate*, Sensors and Actuators A (Physical), Vol.A87, (no.1-2), pp72-7, 2000.
13. J. Jang, S. Wang, S. Pilgrim, W. Schulze, ", Journal of the American Ceramic Society, Vol 83:7, pp 1804-1806, 2002.